MOLECULAR AND CELLULAR BIOLOGY, Apr. 2008, p. 2304–2313 Vol. 28, No. 7
0270-7306/08/$08.00+0 doi:10.1128/MCB.00683-07

Survival Signaling by C-RAF: Mitochondrial Reactive Oxygen Species and Ca^{2+} Are Critical Targets▽

Andrey V. Kuznetsov,[1]† Julija Smigelskaite,[1]† Christine Doblander,[1] Manickam Janakiraman,[1]‡ Martin Hermann,[2] Martin Wurm,[2] Stefan F. Scheidl,[1] Robert Sucher,[1] Andrea Deutschmann,[2] and Jakob Troppmair[1]*

Daniel Swarovski Research Laboratory[1] and KMT Laboratory,[2] Department of General and Transplant Surgery, Innsbruck Medical University, 6020 Innsbruck, Austria

Received 19 April 2007/Returned for modification 23 July 2007/Accepted 26 December 2007

Survival signaling by RAF occurs through largely unknown mechanisms. Here we provide evidence for the first time that RAF controls cell survival by maintaining permissive levels of mitochondrial reactive oxygen species (ROS) and Ca^{2+}. Interleukin-3 (IL-3) withdrawal from 32D cells resulted in ROS production, which was suppressed by activated C-RAF. Oncogenic C-RAF decreased the percentage of apoptotic cells following treatment with staurosporine or the oxidative stress-inducing agent *tert*-butyl hydroperoxide. However, it was also the case that in parental 32D cells growing in the presence of IL-3, inhibition of RAF signaling resulted in elevated mitochondrial ROS and Ca^{2+} levels. Cell death is preceded by a ROS-dependent increase in mitochondrial Ca^{2+}, which was absent from cells expressing transforming C-RAF. Prevention of mitochondrial Ca^{2+} overload after IL-3 deprivation increased cell viability. MEK was essential for the mitochondrial effects of RAF. In summary, our data show that survival control by C-RAF involves controlling ROS production, which otherwise perturbs mitochondrial Ca^{2+} homeostasis.

Apoptosis suppression by C-RAF may involve direct effects on regulators of cell survival and recruitment of effector pathways, which through transcription-dependent and -independent mechanisms suppress apoptotic cell death (37, 43). Like other survival proteins, activated C-RAF maintains mitochondrial membrane integrity; however, the critical targets at the mitochondria remain to be identified. Alterations in mitochondrial reactive oxygen species (ROS) and Ca^{2+} commonly precede cell death. ROS-induced apoptosis implies direct toxic effects, as well as a function of ROS as signaling molecules which trigger the activation of prodeath pathways (38). Mitochondrial respiratory chain complexes I and III (NADH: ubiquinone oxidoreductase and ubiquinone-cytochrome *c* reductase) (12) and plasma membrane-located NAD(P)H oxidases (14) are considered the main sites of cellular superoxide generation. Unphysiologically high mitochondrial Ca^{2+} levels ("mitochondrial Ca^{2+} overload") directly affect mitochondrial permeability for apoptogenic factors and thus cause apoptosis (30). The endoplasmic reticulum (ER) is an important source for this Ca^{2+}, and the Ca^{2+} content of this organelle determines the cell's responsiveness to apoptotic stress. ER Ca^{2+} levels are subject to control by Bcl-2 proteins whereby Bcl-2 decreases the ER Ca^{2+} while proapoptotic BAX and BAK enhance the flow of Ca^{2+} from the ER to the mitochondria (24). Here we demonstrate that the lack of growth factors, a common physiological cell death stimulus, causes increased mitochondrial ROS production and elevated mitochondrial Ca^{2+} levels, which are directly linked to the onset of apoptosis. C-RAF maintains cell survival by controlling mitochondrial ROS and Ca^{2+} through a MEK-dependent mechanism.

MATERIALS AND METHODS

Cell culture. Parental promyeloid interleukin-3 (IL-3)-dependent 32D cells and 32D-vRAF expression-activated C-RAF, AKT, and MEK have been described before (4, 39). The cultivation and processing of cells for all experiments was carried out as previously described (39). Cell viability was routinely assessed using trypan blue exclusion, which correlates with nuclear DNA degradation and DNA loss (4), changes in mitochondrial membrane potential, cytochrome *c* release, and caspase activation (15). UO126 and LY294002 were obtained from Promega and used as previously described (39). The RAF kinase inhibitor BAY43-9006 was a gift from Bayer.

Generation of 32D cells expressing MnSOD, Bcl-2, or OHT-inducible activated C-RAF (BXB). The expression plasmid for human manganese-dependent superoxide dismutase (MnSOD), pcDNA3hMnSOD, was provided by L. Oberley. 32D cells were transfected using nucleofector technology (Amaxa Biosystems, Cologne, Germany) and an established protocol provided by the manufacturer. The expression construct for Bcl-2, pLib-bcl2-iresPuro, was provided by M. J. Ausserlechner. Production of retroviruses and retroviral infection were done as described before (25). Following selection in 1 mg/ml G418 (MnSOD) or 2 μg/ml puromycin (Bcl-2), expression of these proteins was confirmed by Western blotting following established procedures (39). To generate 32D cells expressing a 4-hydroxytamoxifen (OHT)-inducible oncogenic mutant of C-RAF (11), parental 32D cells were transfected with the plasmid pBABE puro BXB-ER (10) by use of the Amaxa nucleofector technology. Following puromycin selection (2 μg/ml), the resulting cell pool was analyzed for OHT-regulated activation of extracellular signal-regulated kinase 1/2 (ERK1/2) and survival and used in the experiments described below.

Immunoblotting. Proteins were detected following a previously published procedure (29). The following proteins were detected by the antibodies indicated in parentheses: BAX (sc-526; Santa Cruz Biotechnology), BAD (9292; Cell Signaling Technology), Bcl-2 (sc-492; Santa Cruz Biotechnology), B-RAF (sc-166; Santa Cruz Biotechnology), C-RAF (sc-133; Santa Cruz Biotechnology), Cu/ZnSOD (SOD-101; Stressgen), GAPDH (AM4300; Ambion), glutathione peroxidase 1 (ab16798; Biozol), MnSOD (06-984; Upstate), AKT1/2 (sc-8312; Santa Cruz Biotechnology), Puma (P4618; Sigma), Bim (AAP-330; Stressgen), Bcl-x

* Corresponding author. Mailing address: Daniel Swarovski Research Laboratory, Department of General and Transplant Surgery, Innsbruck Medical University, Innrain 66, 6020 Innsbruck, Austria. Phone: 43 512 504 24624. Fax: 43 512 504 24625. E-mail: jakob.troppmair@i-med.ac.at.

† These authors contributed equally to this work.

‡ Present address: Department of Medicine, Memorial Sloan-Kettering Cancer Center, New York, NY 10021.

▽ Published ahead of print on 22 January 2008.

(2762; Cell Signaling Technology), pERK (sc-7383; Santa Cruz Biotechnology), ERK (sc-94; Santa Cruz Biotechnology), and MEK (9122; Cell Signaling Technology).

Measurement of ROS production. ROS production was measured by loading cells (approximately 0.5×10^6 cells per ml) washed in phosphate-buffered saline (PBS; Invitrogen, Carlsbad, CA) or medium either with 20 μM DCF-DA (2,7-dichlorodihydrofluorescein diacetate; Molecular Probes, Eugene, OR) for 20 min in the dark or with 5 μM MitoSOX Red (Molecular Probes, Eugene, OR) (23) for 20 min. After being washed with PBS or medium, cells were further processed for analysis by spectrofluorometry or confocal microscopy. Treatment with trolox (6-hydroxy-2,5,7,8-tetramethylchroman-2-carboxylic acid; Sigma, St. Louis, MO), a cell-permeable, water-soluble derivative of vitamin E with potent antioxidant properties, or the direct-acting oxidative stress-inducing agent *tert*-butyl hydroperoxide (*t*-BHP; Sigma, St. Louis, MO) was carried out by directly adding the reagents to the tissue culture medium. The ROS production of DCF-DA- or MitoSOX Red-preloaded cells was measured using a Shimadzu RF-5301PC spectrofluorophotometer, and results are expressed as arbitrary units per number of viable cells. The following settings were used: for DCF-DA, 488 nm excitation and 522 emission; for MitoSOX Red, 510 nm excitation and 580 emission. DCF-DA fluorescence intensity was linearly proportional up to a cell density of 5×10^6 cells per ml (data not shown).

Confocal imaging of mitochondria, ROS, and mitochondrial calcium. Cells were placed in Lab-Tek chambered cover glass (Nalge Nunc, Rochester, NY) with a chamber volume of 0.3 to 0.4 ml at 10×10^3 to 20×10^3 cells per chamber. In order to analyze mitochondrial inner membrane potential, cells were incubated for 30 min with 50 nM tetramethylrhodamine methyl ester (TMRM; Sigma, St. Louis, MO) added directly to the cell culture medium. In control experiments, dissipation of membrane potential was observed after the addition of 5 μM antimycin A (Sigma, St. Louis, MO), 4 μM FCCP (carbonyl cyanide-*p*-trifluoromethoxyphenyl-hydrazone; Sigma, St. Louis, MO), or 0.5 μM rotenone (Sigma, St. Louis, MO) (data not shown). For colocalization studies of mitochondria and ROS, cells were loaded with DCF-DA (20 μM) and TMRM (50 nM) or with MitoTracker Green (0.2 μM; Molecular Probes, Eugene, OR) and MitoSOX Red (5 μM). To analyze the level of mitochondrial matrix calcium, $[Ca^{2+}]_m$, cells were preloaded with fluorescent Ca^{2+}-specific probe Rhod-2 (5 μM; Molecular Probes, Eugene, OR) for 60 min. Rhod-2 has a net positive charge allowing its specific accumulation in mitochondria. In separate experiments, Rhod-2 fluorescence was also analyzed in the presence of trolox (1 mM), different concentrations of *N*-acetylcysteine (NAC; Sigma, St. Louis, MO), thapsigargin (TG, 1.25 μM; Sigma, St. Louis, MO), ruthenium red (RR, 25 μM; Sigma, St. Louis, MO), or BAPTA-AM [1,2-bis-(*o*-aminophenoxy)-ethane-*N*,*N*,*N*′,*N*′-tetraacetic acid, tetraacetoxymethyl ester; Molecular Probes, Eugene, OR]. The digital images of TMRM, DCF-DA, MitoSOX Red, and Rhod-2 fluorescence were taken using an inverted confocal microscope (Leica DM IRE2) with a 63× water immersion lens or with the microlens-enhanced Nipkow disk-based confocal system UltraVIEW RS (Perkin Elmer, Wellesley, MA) mounted on an Olympus IX-70 inverse microscope with a 40× water immersion lens (Olympus, Nagano, Japan). Images were acquired with the UltraVIEW RS software (Perkin Elmer, Wellesley, MA). The DCF-DA fluorescence was excited with the 488-nm line of a laser for excitation and with 505 to 550 nm for emission. TMRM, MitoSOX Red, and Rhod-2 fluorescences were measured using 543 nm for excitation (helium-neon laser) and more than 580 nm for emission. In all cases, quantitative measurements of the fluorescence signal (gray value) were performed using inverted confocal images and Scion Image for Windows software (Scion Corporation, NIH). Data from 30 to 60 cells were averaged after background (no-cell area) fluorescence correction.

siRNA. Transfection of 32D cells was performed using the Amaxa nucleofector kit V following manufacturer's instructions. ON TARGETplus SMARTpool small interfering RNA (siRNA) for mouse C-RAF and B-RAF as well as ON TARGETplus SMARTpool duplex (7) directed against mouse C-RAF was obtained from Dharmacon. The effect of siRNAs on endogenous B- and C-RAF expression was confirmed by immunoblotting. For negative controls, we used microarray-tested siCONTROL nontargeting siRNA 2 (Dharmacon), which according to company information possesses at least four mismatches to any human, mouse, or rat gene.

Total RNA isolation. Ten million cells were incubated for 8 h in the presence or absence of IL-3, collected by centrifugation, washed twice with PBS, and resuspended in 1 ml of TRIzol reagent (Invitrogen, Carlsbad, CA), followed by an incubation step at room temperature for 5 min. Then, 200 μl of chloroform was added, and samples were vortexed thoroughly, incubated for 2 min at room temperature, and then centrifuged at 12,000 × *g* for 5 min at 4°C. The upper phase was transferred to a clean tube and an equal amount of 70% ethanol was added. Then, samples were transferred to RNeasy spin columns (Qiagen, Hilden, Germany) and further processed according to the manufacturer's protocol.

cDNA synthesis and real-time quantitative PCR. First-strand cDNA synthesis was carried using an RT^2 first-strand kit (SuperArray Inc., Bethesda, MD) following the manufacturer's protocol. For cDNA synthesis, 4 μg of total RNA was used. Real-time quantitative PCR was performed using RT^2 real-time SYBR green-fluorescein PCR master mix according to the protocol provided on an iQ5 multicolor real-time PCR detection system (Bio-Rad), and primers were purchased from SuperArray Inc. (Bethesda, MD). The amplification reactions were performed in a final volume of 25 μl using 100 ng of DNA template per reaction. Expression was normalized to a reference gene, the GAPDH gene. The following PCR primers obtained from SuperArray Inc. (Bethesda, MD) were used: those for Bcl-x (PPM02920E), Bim (PPM03429E), Puma (PPM04997A), Cu/ZnSOD (PPM03582A), thioredoxin (PPM35777A), glutathione peroxidase 1 (PPM04345E), catalase-1 (PPM04394B), and GAPDH (PPM02946E).

Each RNA sample was assayed in triplicate and the results are presented as an expression ratio of 32D-vRAF cells against wild-type 32D cells. Data analysis was performed using the $2^{-\Delta\Delta}C^T$ method (C_T is for threshold cycle) (16). Melting curve analysis and agarose gel electrophoresis were done for quality control. Each experiment was repeated three times.

Data analysis. All data are presented as means ± standard deviations. Statistical analyses were performed by *t* test or by using analysis of variance followed by the post hoc test (Tukey multiple-comparisons test) for comparison between individual groups. Significance was considered at a P value of <0.05.

RESULTS

Proapoptotic stimuli cause enhanced ROS production which is prevented by activated C-RAF or IL-3. IL-3 withdrawal readily induces apoptosis of 32D cells (4, 39). ROS production in IL-3-deprived cells was monitored by loading cells with the ROS-sensitive dye DCF-DA (20, 34, 46), and changes in fluorescence were followed up by confocal microscopy (Fig. 1). These experiments demonstrated a substantially increased production of ROS detectable at 8 h, with peak levels observed around 15 h after growth factor removal. Only moderate levels of ROS were detected in cells maintained in the presence of IL-3 (Fig. 1A and B), suggesting the involvement of IL-3 signaling. C-RAF and phosphatidylinositol (PI 3)-kinase/AKT both control survival and proliferation downstream of the IL-3 receptor (39). Expression of an oncogenic mutant of C-RAF, vRAF, was sufficient to significantly delay the onset of apoptosis following IL-3 removal (4). Using 32D cells stably expressing vRAF, we showed that activated RAF prevented the increase in ROS as efficiently as IL-3 (Fig. 1B). This finding suggested that RAF signaling downstream of the IL-3 receptor was critical for maintaining permissive ROS levels. Similar to IL-3 withdrawal, vRAF also protected cells against the dramatically increased ROS production following exposure to staurosporine (STS), a commonly used cell death inducer (Fig. 1B), or exposure to the directly oxidative stress-inducing agent *t*-BHP (data not shown). The protective effect of vRAF was identical to that of IL-3 (Fig. 1B). Notably, the presence of the antioxidant NAC during STS treatment had the same effect as the expression of activated C-RAF (Fig. 1B), supporting the view that in both cases ROS are critical intermediates. Identical results were obtained when MitoSOX Red, a specific mitochondrial superoxide indicator, was used (Fig. 1C and D). Taken together, our data identified ROS as a critical RAF-controlled intermediate in cell death induction.

Increased mitochondrial ROS production is linked to cell death induction. Treatment of cells with the oxidative stress-inducing agent *t*-BHP raised cellular ROS levels (data not shown) and significantly increased the fraction of apoptotic

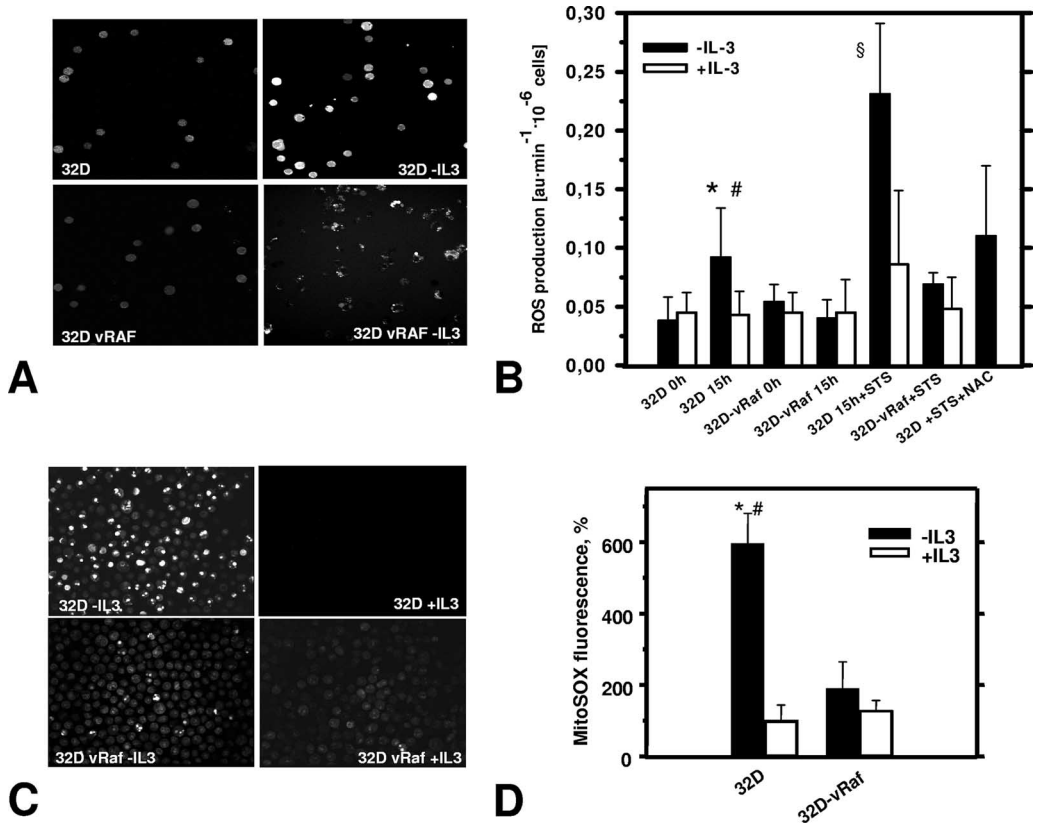

FIG. 1. Cell death induction results in enhanced ROS production which is suppressed by IL-3 or activated RAF. (A) Representative confocal images of DCF-DA-loaded cells show that IL-3 deprivation of 32D cells (8 to 9 h) triggers release of ROS, as detected by a significant increase of DCF-DA fluorescence (top), which is suppressed by activated C-RAF (vRAF) (bottom). (B) Summary of spectrofluorophotometric ROS measurements (DCF-DA labeling experiments). In addition to its protective effect during IL-3 deprivation (15 h), vRAF protects against STS-induced ROS production (STS concentration, 5 nM), which can also be inhibited by antioxidant NAC (20 mM). Symbols: ∗, significantly different from 32D cells plus IL-3 ($P < 0.001$; $n = 9$); #, significantly different from vRAF cells ($P < 0.01$; $n = 7$ to 9); §, significantly different from plus-IL-3 and vRAF groups ($P < 0.01$; $n = 4$). au, arbitrary units. (C) Representative confocal images of intracellular ROS in cells preloaded with specific mitochondrial superoxide indicator MitoSOX Red (5 μM) demonstrate results of increased ROS levels and protective effects of vRAF similar to those seen for DCF-DA (panel A). (D) Statistical analysis of MitoSOX Red fluorescence intensity. ROS probe MitoSOX Red confirms results obtained with DCF-DA and suggests a mitochondrial origin of ROS. 32D and 32D-vRAF cells were deprived of IL-3 through extensive washing and set up at a density of 0.5×10^6/ml. Then, 15 to 16 h later, cells were labeled with MitoSOX Red. The fluorescence signal was quantified using Scion Image software as described in Materials and Methods. Symbols: ∗, significantly different from control (+IL-3); #, significantly different from vRAF (−IL-3) ($P < 0.001$; $n = 4$ to 6).

cells (Fig. 2). The presence of NAC lowered ROS levels (Fig. 1B) and reduced the number of apoptotic cells (Fig. 2). These experiments demonstrated that increased intracellular ROS directly resulted in apoptosis in the case of IL-3 deprivation and STS or prooxidant treatments.

To further confirm the mitochondrial origin of ROS, we used the specific mitochondrial markers TMRM (red) and MitoTracker Green (Fig. 3A, top). Confocal imaging of DCF-DA (green) and the mitochondrial inner membrane potential-sensitive dye TMRM (red) demonstrated the spatial colocalization of ROS following IL withdrawal and mitochondria (Fig. 3A, middle). A similar staining pattern (colocalization) was also observed for two different ROS probes, DCF-DA and MitoSOX Red (Fig. 3A, bottom).

The uncoupling reagents FCCP and 2,4-dinitrophenol (DNP) partially eliminate the mitochondrial membrane potential by allowing protons to leave across the mitochondrial membrane. Treatment of cells with low concentrations of un-

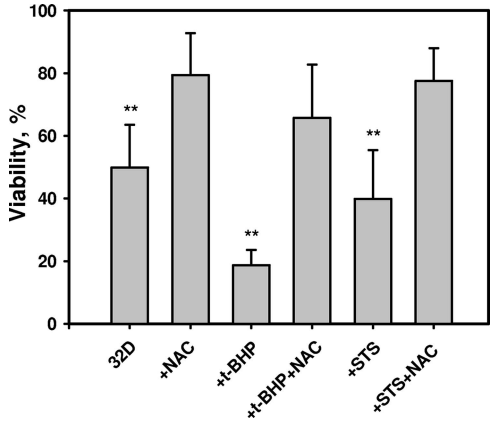

FIG. 2. Pro- and antioxidant control of 32D cell survival. 32D cells were deprived of IL-3 and cell viability was determined as described in Materials and Methods. NAC demonstrates significant cell protection under conditions of IL-3 deprivation, oxidative stress induced by the direct prooxidant *t*-BHP, and STS-induced apoptosis. ∗∗, significantly different from corresponding groups with NAC ($P < 0.001$; $n = 3$).

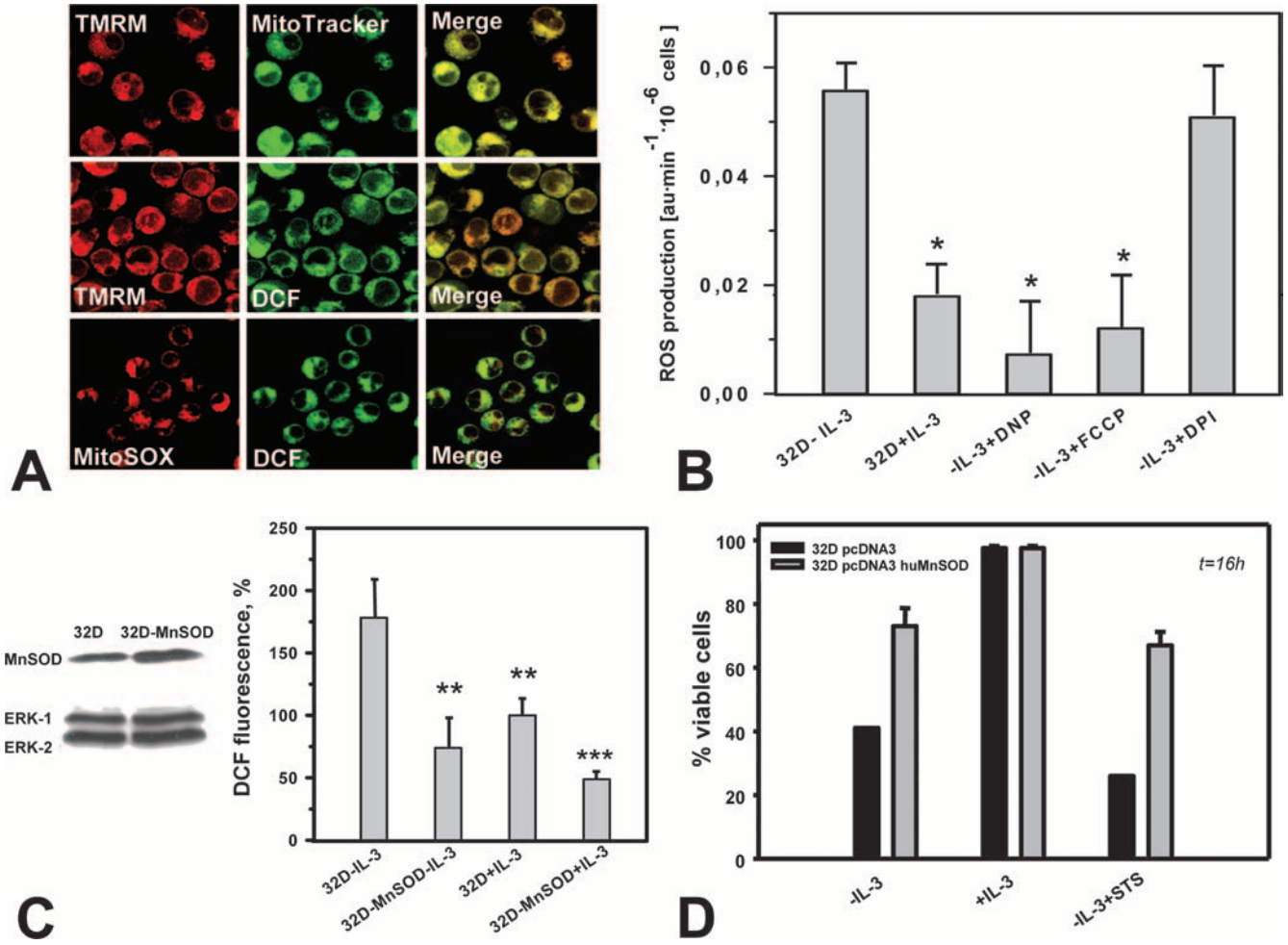

FIG. 3. ROS production in IL-3-deprived 32D cells occurs primarily at mitochondrial sites. (A) The mitochondrial membrane potential-sensitive dye TMRM fully colocalized with the mitochondrial marker MitoTracker Green (top) but also with DCF-DA fluorescence (green) (middle). Visualization of ROS by the superoxide-specific indicator MitoSOX Red (red) demonstrated colocalization with ROS as detected by DCF-DA (DCF) (bottom). (B) Treatment with either of the mitochondrial uncouplers FCCP (5 nM) and DNP (2 μM) was associated with significantly reduced ROS production ($P < 0.05$; $n = 3$), whereas the inhibitor of NADPH oxidase diphenyleneiodonium chloride (DPI) (1 μM) had no effect. au, arbitrary units. (C) Western blot analysis of MnSOD-transfected 32D cells shows elevated expression of MnSOD (left). MnSOD overexpression significantly protects growth factor-deprived 32D cells from excessive ROS production as measured by DCF-DA (DCF) fluorescence (percent control 32D-plus-IL-3 cells [right]). Symbols: **, $P < 0.01$; ***, $P < 0.001$ ($n = 3$). (D) MnSOD overexpression protects 32D cells from cell death induced by IL-3 withdrawal or by STS (7.5 nM).

couplers ("mild" uncoupling) normally decreases mitochondrial ROS production (21). Incubation with low concentrations of FCCP or DNP significantly reduced ROS production in IL-3-deprived 32D cells, whereas the commonly used NAD(P)H oxidase inhibitor diphenyleneiodonium chloride had no effect on ROS levels (Fig. 3B), supporting a mitochondrial origin of ROS.

SODs convert superoxide radicals into hydrogen peroxide (H_2O_2), which can be further transformed into the highly reactive hydroxyl radical or into water and oxygen by catalase or glutathione peroxidase (6). Introduction of an MnSOD expression plasmid in 32D cells resulted in only a moderate increase in MnSOD levels but caused (i) a significantly reduced ROS production as measured by DCF-DA fluorescence (Fig. 3C) and (ii) a decrease in the number of apoptotic cells induced by growth factor withdrawal or by STS (Fig. 3D). These experiments further confirm the mitochondria as the source of ROS and additionally confirm the critical role of ROS as a trigger of apoptotic cell death. The antiapoptotic potential of overexpressed MnSOD in these cells was comparable to the effects of activated RAF.

Apoptosis induced by growth factor withdrawal is associated with increased mitochondrial Ca^{2+} levels. Mitochondrial Ca^{2+} overload leads to apoptotic cell death and thus may constitute a common end point for many apoptosis triggers (30). Using Rhod-2 to monitor mitochondrial Ca^{2+} levels, we demonstrated that growth factor withdrawal resulted in a significant increase of mitochondrial Ca^{2+} compared to what was seen for nonstarved 32D cells (Fig. 4A). IL-3 or activated C-RAF again prevented this change in mitochondrial Ca^{2+}. A short-term treatment of 32D cells with H_2O_2 (for up to 20 min) caused a remarkable increase in mitochondrial Ca^{2+} (Fig. 4A′), sug-

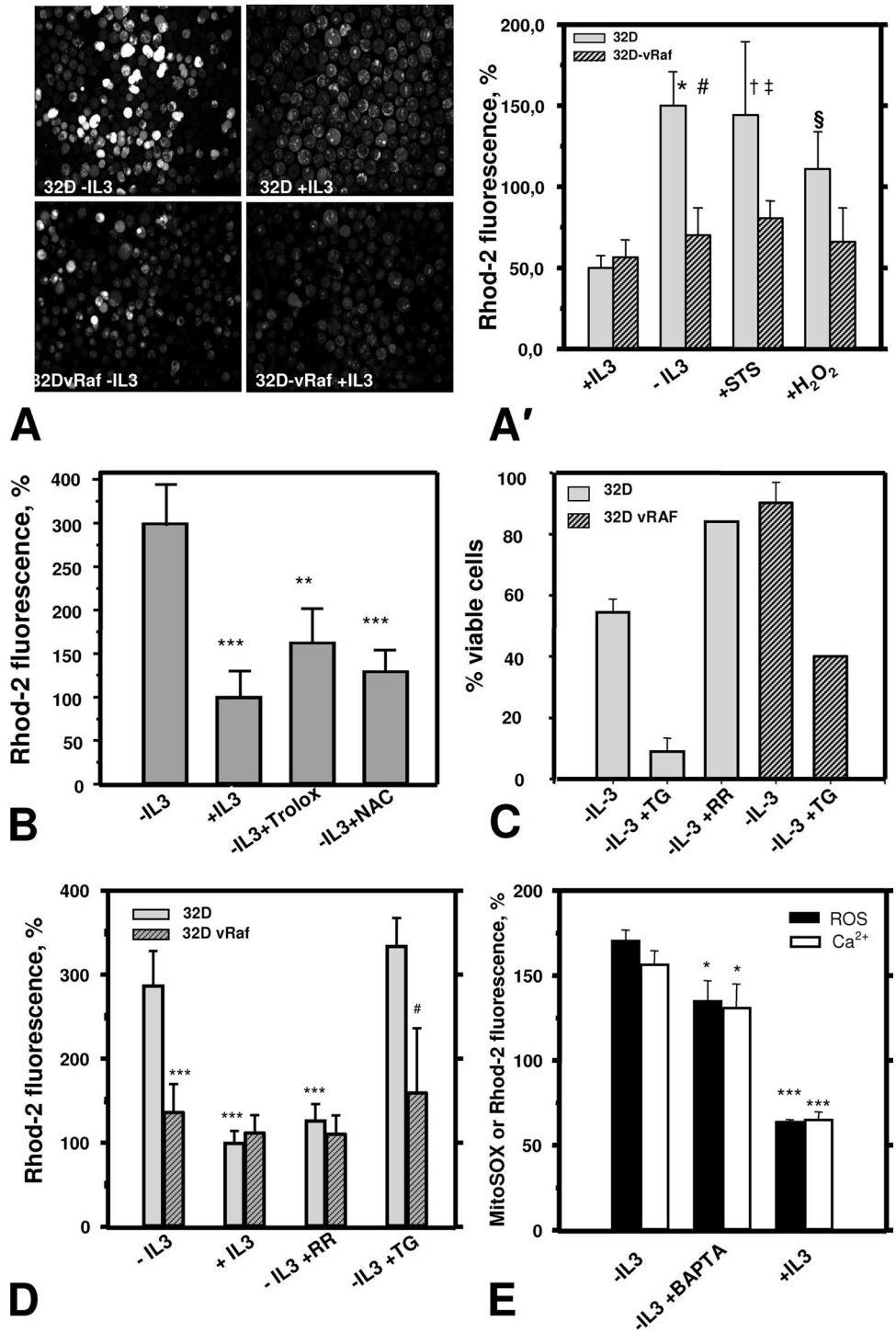

FIG. 4. Mitochondrial Ca^{2+} is involved in ROS-induced cell death. (A and A′) Growth factor withdrawal results in a ROS-dependent increase in mitochondrial Ca^{2+}. Cells preloaded with specific probe Rhod-2 (5 μM) were used to monitor mitochondrial Ca^{2+} levels following IL-3 deprivation and under conditions of oxidative stress (H_2O_2) or STS-induced apoptosis. (A) Representative confocal images of Rhod-2 fluorescence. (A′) Summary of the quantitative analysis of Rhod-2 imaging. The significant increase in mitochondrial Ca^{2+} after IL-3 withdrawal was similar to the effects of STS treatment or direct oxidant H_2O_2 (500 μM) and was markedly suppressed through activated RAF (32D-vRAF). Symbols: ∗, significantly different from control 32D-plus-IL-3 cells ($P < 0.001$; $n = 8$); #, significantly different from 32D-vRAF, IL-3-deprived cells ($P < 0.001$; $n = 8$); †, significantly different from control 32D-plus-IL-3 cells ($P < 0.001$; $n = 4$ to 8); ‡, significantly different from STS-treated 32D-vRAF cells ($P < 0.05$; $n = 4$); §, significantly different from control 32D-plus-IL-3 cells ($P < 0.001$; $n = 5$ to 8). (B) Increase in mitochondrial Ca^{2+} (Rhod-2 fluorescence intensity) in IL-3-deprived 32D cells is significantly suppressed by antioxidants trolox (1 mM) and NAC (20 mM). ∗∗ and ∗∗∗, significantly different from IL-3-deprived 32D cells ($P < 0.01$ and $P < 0.001$, respectively). (C) Mitochondrial Ca^{2+} affects cell viability. TG treatment (1.25 μM) is associated with cell death in parental 32D cells but this was much less so for 32D cells protected by activated RAF. In the presence of IL-3, we observed a decrease in cell viability by 13% in the case of 32D-vRAF cells and 17% for 32D cells (average from two

gesting that the changes observed are linked to oxidative stress. Again, the effect of H_2O_2 was almost abolished in cells protected by vRAF (Fig. 4A′). As shown before for cell survival and ROS, the presence of the antioxidants NAC or trolox significantly reduced the mitochondrial Ca^{2+} overload in growth factor-starved cells (Fig. 4B). Taken together, these findings suggest a sequence of events in which ROS production is required for and most likely precedes the increase in mitochondrial Ca^{2+} observed in this study.

RR blocks mitochondrial Ca^{2+} uptake via inhibition of the mitochondrial uniporter (42). As shown in Fig. 4C and D, RR efficiently protected cells against apoptosis (Fig. 4C) and mitochondrial Ca^{2+} overload (Fig. 4D), demonstrating that mitochondrial Ca^{2+} uptake mechanisms are involved. Again, under conditions of IL-3 deprivation, RR and activated C-RAF displayed very similar protective effects (Fig. 4C and D). Moreover, treatment with RR substantially prevented excessive ROS production in our model (data not shown). A similar effect, much less pronounced but still significant, was observed when the intracellular Ca^{2+} chelator BAPTA-AM was used (Fig. 4E). This treatment also lowered the cytoplasmic Ca^{2+} level, as shown by Fura Red labeling (data not shown). BAPTA treatment also improved the viability of IL-3-deprived cells (41.7% ± 5.2% [control] versus 76.5% ± 2.9% [BAPTA-AM-treated cells]).

TG (35), a specific inhibitor of ER Ca^{2+}ATPase (2, 35), blocks ER Ca^{2+} uptake, thereby increasing cytosolic Ca^{2+}, which may cause concomitant mitochondrial Ca^{2+} overload (33, 45). TG treatment of 32D cells elevated Ca^{2+} levels in mitochondria and increased the number of apoptotic cells (Fig. 4C and D). Again, these effects of TG were prevented by activated C-RAF.

Requirement for RAF, MEK, and AKT in maintaining ROS and Ca^{2+} homeostasis by IL-3. To get a more general understanding regarding the role of RAF signaling in the control of mitochondrial events, we also analyzed the effect of interfering with RAF signaling in parental 32D cells growing in the presence of IL-3. To this end, we used two different approaches: inhibition with the RAF-specific inhibitor BAY43-9006 and conditional knockdown using siRNA targeting RAF. 32D cells growing in IL-3 were incubated for 48 h with the RAF inhibitor and then analyzed for changes in ROS and Ca^{2+}. The presence of 15 μM BAY43-9006 resulted in increased production of ROS and elevated mitochondrial Ca^{2+} levels (Fig. 5A). A similar effect was observed with the MEK inhibitor U0126, suggesting a MEK requirement downstream of RAF. We have shown previously that the PI 3-kinase inhibitor LY294002 had the same effect on proliferation and survival of 32D cells as U0126 (39). Blocking PI 3-kinase activity also resulted in enhanced mitochondrial ROS production (Fig. 5A), suggesting that mitochondrial alterations occurring in IL-3-starved 32D cells are also controlled by this pathway.

We next tested the effect of conditionally knocking down RAF in 32D cells growing in IL-3. Since both C- and B-RAF are expressed in 32D cells and have been implicated in the propagation of mitogenic and survival signals (43), we independently targeted them (Fig. 5B, inset). Ablation of both C-RAF and B-RAF resulted in ROS production, together with increased mitochondrial Ca^{2+} levels, with B-RAF inhibition showing a more pronounced effect (Fig. 5B). These data confirm that RAF kinases are also involved in mitochondrial control during normal growth factor signaling and point to a role for B-RAF in this process.

As reported earlier (39), the survival activity of vRAF in 32D cells was severely compromised by inhibiting MEK or PI 3-kinase activity. In agreement with the postulated role of ROS and Ca^{2+} in the induction of apoptosis in these cells, these inhibitors also caused an increase in mitochondrial ROS and Ca^{2+} levels (Fig. 5C). The effect of inhibiting MEK in 32D-vRAF cells deprived of IL-3 was comparable to that of inhibiting RAF, demonstrating again the critical role of this effector. This was also directly addressed by analyzing cells expressing constitutively active MEK, as described before (39). As shown in Fig. 6, MEK efficiently suppressed mitochondrial changes in ROS and Ca^{2+} in the absence of growth factor with a potency similar to that of vRAF.

We have previously identified the requirement of AKT downstream of PI 3-kinase in mediating cell survival in these cells (39). We thus also examined 32D cells expressing activated AKT (Fig. 6B) for the effect on ROS production and mitochondrial Ca^{2+} levels and again observed a protective effect (Fig. 6A). We also have shown in the past that oncogenic RAF was able to protect Bcl-2-deficient cells, while Bcl-2 similarly protected cells lacking C-RAF from apoptosis (44). We therefore also tested Bcl-2 and found that Bcl-2 also controlled mitochondrial ROS and Ca^{2+} (Fig. 6). These data suggest that major prosurvival pathways are able to control mitochondrial Ca^{2+} and ROS homeostasis, supporting the critical role of these second messengers in regulating life/death decisions.

To exclude the possibility that the RAF effects observed here with stably transfected cell lines require additional changes, we generated 32D cells expressing a hormone-regulated version of activated RAF described previously (10, 11). Like vRAF, this mutant of RAF possesses transformation potential and efficiently activates ERK1/2 (10, 11). In our experiments, it demonstrated ERK1/2 activation (Fig. 5D) and survival potential (24-h survival in the absence of IL-3; 29.6% ± 0.7% [without OHT] versus 68.1% ± 2.6% [with OHT]). As shown in Fig. 5D, conditional activation of RAF was sufficient

experiments). (D) TG (1.25 μM) causes mitochondrial Ca^{2+} overload, which is suppressed by activated RAF. RR (50 μM) prevented Ca^{2+} overload, also displaying clear prosurvival activity (panel C). Symbols: ***, significantly different from IL-3-deprived 32D cells ($P < 0.001$, $n = 4$); #, significantly different from the 32D-plus-TG cell group ($P < 0.05$; $n = 4$ or 5). (E) BAPTA-AM (10 μM), an intracellular calcium chelator, diminishes the increase in mitochondrial ROS and Ca^{2+} caused by growth factor deprivation. Cells incubated for 16 h in the presence of BAPTA-AM or dimethyl sulfoxide (DMSO; vehicle) were preloaded with specific probe MitoSOX Red (5 μM) or Rhod-2 (5 μM) and used to monitor mitochondrial ROS or Ca^{2+} levels, respectively. * and ***, significantly different from the IL-3-deprived sample ($P < 0.05$ and $P < 0.001$, respectively; $n = 3$).

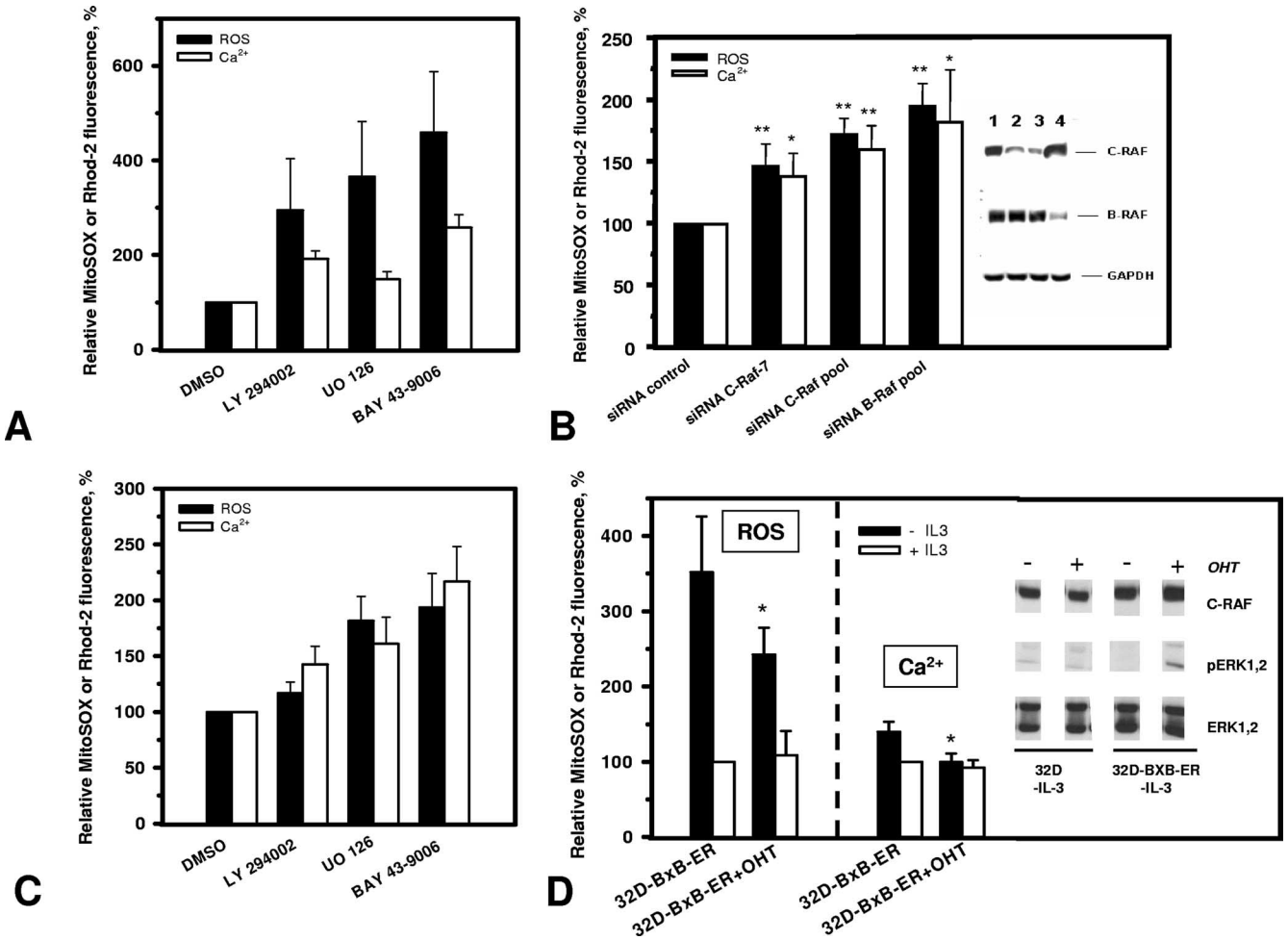

FIG. 5. Requirement of RAF kinases in maintaining ROS and Ca^{2+} homeostasis. ROS and Ca^{2+} analyses were performed loading cells with specific probes MitoSOX Red (5 μM) and Rhod-2 (5 μM), respectively. (A) Inhibition of PI 3-kinase, MEK, and RAF increases mitochondrial ROS and Ca^{2+} levels in 32D cells growing in the presence of IL-3. Cells were incubated with specific inhibitors LY294002 (25 μM), UO126 (25 μM), and BAY43-9006 (15 μM) for PI 3-kinase, MEK, and RAF, respectively, or with DMSO (vehicle) for 48 h and then analyzed for mitochondrial ROS and Ca^{2+} levels. (B) RAF knockdown with siRNA in 32D cells growing in the presence of IL-3 significantly augments ROS and Ca^{2+} levels. 32D cells were transfected with control siRNA, C-RAF duplex 7 siRNA, C-RAF pool siRNA, and B-RAF pool siRNA (lanes 1, 2, 3, and 4, respectively, in the immunoblot) as described in Materials and Methods. Cells were analyzed for protein expression and ROS and Ca^{2+} levels 48 h after transfection. * and **, significantly different from siRNA control sample ($P < 0.05$ and $P < 0.01$, respectively; $n = 3$). (C) Inhibition of MEK or RAF remarkably increases mitochondrial ROS and Ca^{2+} levels in 32D-vRAF cells deprived of IL-3. Inhibition of PI 3-kinase also causes a less pronounced increase. Cells were incubated with the specific inhibitors LY294002 (25 μM), UO126 (25 μM), and BAY43-9006 (15 μM) for PI 3-kinase, MEK, and RAF, respectively, or with DMSO (vehicle) for 16 h and then analyzed for mitochondrial ROS and Ca^{2+} levels. (D) Induction of RAF protects IL-3-deprived 32D cells from elevation of mitochondrial ROS and Ca^{2+}. 32D-BXB-ER cells were grown in the absence or presence of OHT (200 nM) for 40 h and during the subsequent 16 h kept with or without IL-3 and then analyzed for ROS and Ca^{2+}. *, significantly different from cells cultured without OHT ($P < 0.05$; $n = 3$ or 4). (Inset) parental 32D cells or 32D-BXB-ER cells were grown in the presence or absence of IL-3 for 8 h and during this time either were left untreated or were incubated with OHT (200 nM) and afterward were analyzed for phosphorylation of ERK1/2 and the expression of total ERK1/2 and C-RAF.

to prevent alterations in mitochondrial ROS and Ca^{2+} elicited through IL-3 withdrawal.

Role of Bcl-2 family proteins and antioxidant systems in the mediation of mitochondrial control by RAF. To address the possibility that the effects of RAF are mediated via Bcl-2 family members (31) or the upregulation of enzyme systems involved in the detoxification of ROS (9), real-time quantitative PCR and immunoblotting were performed. The data from these experiments are summarized in Table 1 and Fig. 7. For expression analysis, we compared 32D cells to 32D-vRAF cells following an 8-h starvation to avoid signaling induced by growth factors. Of the representatives of the Bcl-2 family and of the major antioxidant systems analyzed, none showed any striking changes in expression levels between parental 32D cells and vRAF-expressing cells.

DISCUSSION

Here we identified ROS as essential intermediates which turned the prolonged lack of growth factor into an apoptotic stimulus that could be suppressed by wild-type and activated RAF. Our data also suggested mitochondrial Ca^{2+} overload as

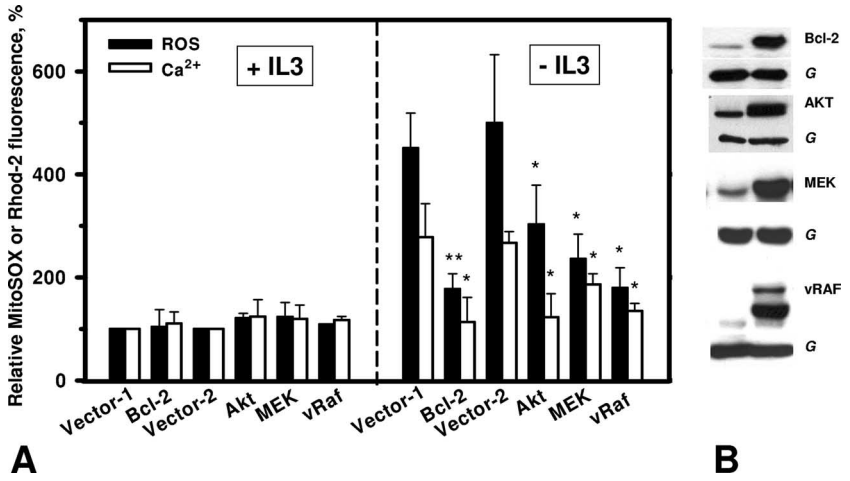

FIG. 6. Expression of activated AKT; MEK or Bcl-2 protects IL-3-deprived 32D cells from elevation of mitochondrial ROS and Ca^{2+}. (A) Cells were deprived of IL-3 through extensive washing and 15 to 16 h later were labeled with MitoSOX Red or Rhod-2. * and **, significantly different from corresponding vector values ($P < 0.05$ and $P < 0.01$, respectively; $n = 3$). (B). 32D Bcl-2, AKT, MEK, and vRAF cells and the corresponding vector cells (*G* [GAPDH]) were washed two times with PBS and directly lysed in Laemmli buffer and processed for immunoblotting as described in Materials and Methods.

a possible mechanism which turned the generation of ROS into cell death (Fig. 8). A central role for ROS in cell death induction is increasingly substantiated by work with different cell models and for various modes of cell death induction, including apoptosis caused by tumor necrosis factor alpha (8) or by serum deprivation from various human and murine cells and cell lines (27) and pancreatic β-cells (18). Various approaches were used in our study to confirm the critical involvement of ROS in 32D cell death. The presence of the radical scavenger NAC during the starvation of 32D cells resulted in prolonged survival, whereas cell death was enhanced through the addition of the direct prooxidant *t*-BHP or the apoptosis inducer STS (Fig. 2). Finally, MnSOD overexpression in 32D cells efficiently protected cells against ROS-induced cell death. Immunoblotting established the expression of MnSOD in parental 32D cells, which was further increased in transfected cells (Fig. 3C and D). The degree of protection offered by increasing MnSOD expression equaled the effects of vRAF or Bcl-2 (1, 4). One possible explanation for our observation is the transcriptional upregulation of protective factors in the cells expressing oncogenic RAF. While certainly limited, our data do not point to an increased expression of antioxidant systems in these cells (Fig. 7; Table 1). Also, the total specific activity levels of catalase were identical in parental and 32D-vRAF cells (data not shown). We also failed to detect any direct effect of vRAF on the expression of various Bcl-2 family members (Fig. 7; Table 1), which are critically involved in the mitochondrial pathway of cell death induction (31).

Theoretically, RAF also may regulate ROS levels by targeting the mitochondrial sites and enzyme systems, where ROS production predominantly occurs (13). The tyrosine kinase SRC, which has been implicated in signaling upstream of C-RAF (5, 36), can phosphorylate and activate cytochrome *c* oxidase, the terminal enzyme in the mitochondrial respiratory chain that catalyzes the reduction of O_2 to H_2O (22). The effect on ROS production has not been analyzed in this context, but reduced cytochrome *c* oxidase activity as a result of genetically

TABLE 1. Relative quantification of real-time quantitative PCR results by the $2^{-\Delta\Delta CT}$ method[a]

Gene	Expression (fold change ± SD)
Bcl-x	2.14 ± 1.65
Bim	1.21 ± 0.67
Puma	1.21 ± 0.32
Cu/ZnSOD	0.83 ± 0.37
Thioredoxin 1	2.48 ± 0.7
Glutathione peroxidase 1	0.99 ± 0.34
Catalase	1.5 ± 1.1

[a] Data are shown as the change in gene expression by 32D-vRAF cells against that by 32D cells. ΔC_T values were obtained by normalization of data to the *GAPDH* reference gene.

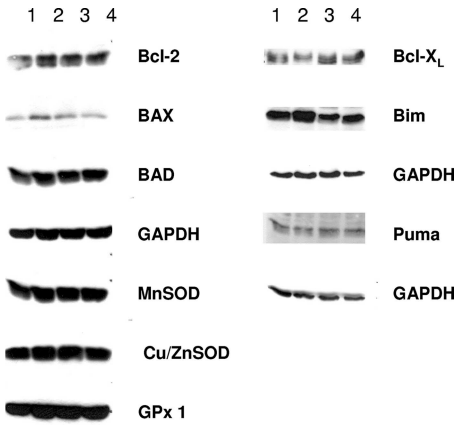

FIG. 7. Effect of oncogenic RAF on the expression of Bcl-2 and antioxidant proteins. 32D and 32D-vRAF cells were incubated with or without IL-3 for 8 h and then washed two times with PBS, directly lysed in Laemmli buffer, and processed for immunoblotting as described in Materials and Methods. Lanes: 1, 32D minus IL-3; 2, 32D plus IL-3; 3, 32D-vRAF minus IL-3; 4, 32D-vRAF plus IL-3.

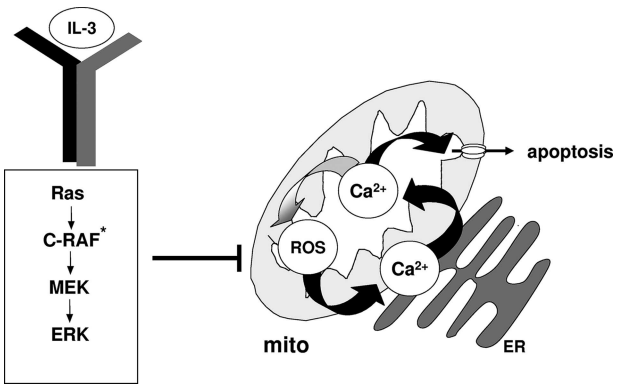

FIG. 8. Mitochondrial events controlled by RAF signaling. Apoptosis of 32D cells induced through the removal of the essential growth and survival factor IL-3 is preceded by an increase in mitochondrial ROS production. This in turn translates into significantly elevated mitochondrial Ca^{2+} levels, which may directly trigger cell death. An increase in mitochondrial Ca^{2+} also may function as a stimulator of ROS production. Changes in mitochondrial Ca^{2+} and ROS levels are prevented by IL-3, antioxidants, or vRAF. mito, mitochondrion. C-RAF*, activated C-RAF.

caused dysfunction (26) or inhibitory phosphorylation by protein kinase A has been correlated with vastly increased ROS production (28). Data presented here do not support the requirement for the physical presence of RAF at the mitochondria to regulate ROS and Ca^{2+} levels but rather point to the critical involvement of the RAF effector MEK (Fig. 5C and 6).

A critical link between apoptotic cell death and mitochondrial Ca^{2+} overload has been worked out in the past (30), and cross talk between ROS and Ca^{2+} may occur at many levels (3, 41). Multiple effects of ROS on intracellular targets have been reported. ROS can directly damage lipids, protein, and DNA, and equally important may be their role in redox signaling (6, 7). Our own experiments suggest that mitochondrial Ca^{2+} levels as well are subject to regulation by ROS and that mitochondrial Ca^{2+} overload may represent the end point in ROS-induced cell killing. Such a mechanism has been observed previously for H_2O_2-induced apoptosis of mouse embryonic fibroblasts (33) or for ROS generated in endothelial cells during ischemia and reperfusion (17). Cellular uptake and shuttling of Ca^{2+} between intracellular stores and the mitochondria are the critical processes regulating Ca^{2+} signaling. Disturbances in these processes can result in cell death. Unphysiologically high matrix Ca^{2+} levels lead to mitochondrial swelling and rupture and permeability transition in the mitochondrial membrane, resulting in the release of factors into the cytoplasm which are required for caspase activation. Mechanisms which provide a mechanistic insight into how ROS may lead to the upregulation of mitochondrial Ca^{2+} have been shown in the past (3). The alterations described above require Ca^{2+} fluxes which are regulated, e.g., through the activity of membrane channels and pumps, which themselves may be affected by ROS (41). Release of Ca^{2+}, in particular from the ER, also has been shown to be subject to regulation by Bcl-2 family members (33). It thus may turn out that the ER-mitochondrion interface provides a critical convergence point for pro- and antiapoptotic signaling.

The data obtained in our study are most consistent with a mitochondrial origin of ROS (Fig. 3A and B). They also point to a sequence of events in which ROS production precedes the increase of mitochondrial Ca^{2+} levels (Fig. 8), while much evidence has been presented for the regulation of intracellular ROS by Ca^{2+} (3). The experimental approach used here, however, does not allow for resolution of the complete sequence of events. It is possible that small changes in mitochondrial Ca^{2+} trigger the sequence of events which increase mitochondrial ROS production, which in turn may amplify mitochondrial Ca^{2+} uptake, thereby triggering a positive-feedback loop.

One main remaining question concerns the mechanisms by which RAF links to the mitochondrial effects described here. Evidence has been provided in the past suggesting that C-RAF may localize to the outer mitochondrial membrane (40). However, our previous work with 32D cells expressing oncogenic RAF demonstrated a requirement for MEK and AKT downstream of RAF for survival signaling (39). The existence of such a survival pathway has been confirmed independently for epithelial cells (32). In our current analyses, we also have included MEK and demonstrated through the use of a specific MEK inhibitor as well as a constitutively active MEK mutant that this kinase potently represses changes in mitochondrial ROS and Ca^{2+} occurring after IL-3 withdrawal (Fig. 5A and C and 6A). We thus postulate that MEK constitutes an essential effector for RAF in this process. The involvement of RAF and MEK can also be demonstrated for 32D cells growing in IL-3 through the use of specific inhibitors and, in the case of C- and B-RAF, also through conditional knockdown of the proteins (Fig. 5A and B). For B-RAF, which was as efficient as C-RAF, evidence for the requirement of mitochondrial localization for survival is missing, and experiments using mitochondrion-targeted active RAF failed to demonstrate the activation of MEK/ERK (40). Taken together, our findings are most consistent with the requirement of a cytoplasmic RAF-MEK-ERK signaling module for survival signaling by wild-type as well as activated RAF kinases.

RAF shares the ability to suppress mitochondrial alterations with AKT (Fig. 6A). Recently, it has been shown that activation of glycogen synthase kinase-3 following the cessation of signal flow through the IL-3 receptor, PI 3-kinase, and AKT resulted in the phosphorylation of the antiapoptotic protein Mcl-1, which targeted it for ubiquitination and subsequent degradation followed by mitochondrial translocation of BAX/BAK (19). This work thus establishes a link between the IL-3 receptor and the permeabilization of the mitochondrial membrane, with a similar critical function in life/death decisions, as shown for mitochondrially produced ROS here. A connection between oncogenic RAF and AKT activation has been established for these cells before (39), and here we show that AKT is also involved in controlling mitochondrial ROS and Ca^{2+} levels (Fig. 5A and C and 6A), while Mcl-1 is degraded in vRAF-expressing cells (J. Smigelskaite, S. Scheidl, and J. Troppmair, unpublished data). Further experiments will thus dissect the cooperation of RAF signaling with other prosurvival molecules to control life/death decisions at the mitochondria.

ACKNOWLEDGMENTS

We thank Eugen Kerkhoff, Larry Oberley, and Michael J. Ausserlechner for providing expression constructs. The excellent technical

support in performing these experiments by Astrid Drasche, Tina Goebel, Anna Draxl, and Daniela Pirkebner is greatly appreciated. We acknowledge the valuable assistance of Ruth Baldauf in the preparation of the manuscript.

Funding for this work was provided by the FWF (MCBO-Sub08), the DFG (GZ, TR 348/2-2), Österreichische Krebshilfe-Krebsgesellschaft Tirol, MFF Tirol (no. 91), TWF (0401/334), and Uniqa Versicherungen AG.

REFERENCES

1. **Baffy, G., T. Miyashita, J. R. Williamson, and J. C. Reed.** 1993. Apoptosis induced by withdrawal of interleukin-3 (IL-3) from an IL-3-dependent hematopoietic cell line is associated with repartitioning of intracellular calcium and is blocked by enforced Bcl-2 oncoprotein production. J. Biol. Chem. **268:**6511–6519.
2. **Bian, J. H., T. K. Ghosh, J. C. Wang, and D. L. Gill.** 1991. Identification of intracellular calcium pools. Selective modification by thapsigargin. J. Biol. Chem. **266:**8801–8806.
3. **Brookes, P. S., Y. Yoon, J. L. Robotham, M. W. Anders, and S. S. Sheu.** 2004. Calcium, ATP, and ROS: a mitochondrial love-hate triangle. Am. J. Physiol. Cell Physiol. **287:**C817–933.
4. **Cleveland, J. L., J. Troppmair, G. Packham, D. S. Askew, P. Lloyd, M. Gonzalez-Garcia, G. Nunez, J. N. Ihle, and U. R. Rapp.** 1994. v-raf suppresses apoptosis and promotes growth of interleukin-3-dependent myeloid cells. Oncogene **9:**2217–2226.
5. **Daum, G., I. Eisenmann-Tappe, H. W. Fries, J. Troppmair, and U. R. Rapp.** 1994. The ins and outs of Raf kinases. Trends Biochem. Sci. **19:**474–480.
6. **Droge, W.** 2002. Free radicals in the physiological control of cell function. Physiol. Rev. **82:**47–95.
7. **Fleury, C., B. Mignotte, and J. L. Vayssiere.** 2002. Mitochondrial reactive oxygen species in cell death signaling. Biochimie **84:**131–141.
8. **Kamata, H., S. Honda, S. Maeda, L. Chang, H. Hirata, and M. Karin.** 2005. Reactive oxygen species promote TNFalpha-induced death and sustained JNK activation by inhibiting MAP kinase phosphatases. Cell **120:**649–661.
9. **Karihtala, P., and Y. Soini.** 2007. Reactive oxygen species and antioxidant mechanisms in human tissues and their relation to malignancies. APMIS **115:**81–103.
10. **Kerkhoff, E., and U. R. Rapp.** 1998. High-intensity Raf signals convert mitotic cell cycling into cellular growth. Cancer Res. **58:**1636–1640.
11. **Kerkhoff, E., and U. R. Rapp.** 1997. Induction of cell proliferation in quiescent NIH 3T3 cells by oncogenic c-Raf-1. Mol. Cell. Biol. **17:**2576–2586.
12. **Kudin, A. P., N. Y. Bimpong-Buta, S. Vielhaber, C. E. Elger, and W. S. Kunz.** 2004. Characterization of superoxide-producing sites in isolated brain mitochondria. J. Biol. Chem. **279:**4127–4135.
13. **Kuznetsov, A. V., M. Janakiraman, R. Margreiter, and J. Troppmair.** 2004. Regulating cell survival by controlling cellular energy production: novel functions for ancient signaling pathways? FEBS Lett. **577:**1–4.
14. **Lambeth, J. D.** 2004. NOX enzymes and the biology of reactive oxygen. Nat. Rev. Immunol. **4:**181–189.
15. **Le Mellay, V., J. Troppmair, R. Benz, and U. R. Rapp.** 2002. Negative regulation of mitochondrial VDAC channels by C-Raf kinase. BMC Cell Biol. **3:**14.
16. **Livak, K. J., and T. D. Schmittgen.** 2001. Analysis of relative gene expression data using real-time quantitative PCR and the 2(-delta delta C(T)) method. Methods **25:**402–408.
17. **Madesh, M., B. J. Hawkins, T. Milovanova, C. D. Bhanumathy, S. K. Joseph, S. P. Ramachandrarao, K. Sharma, T. Kurosaki, and A. B. Fisher.** 2005. Selective role for superoxide in InsP3 receptor-mediated mitochondrial dysfunction and endothelial apoptosis. J. Cell Biol. **170:**1079–1090.
18. **Maestre, I., J. Jordan, S. Calvo, J. A. Reig, V. Cena, B. Soria, M. Prentki, and E. Roche.** 2003. Mitochondrial dysfunction is involved in apoptosis induced by serum withdrawal and fatty acids in the beta-cell line INS-1. Endocrinology **144:**335–345.
19. **Maurer, U., C. Charvet, A. S. Wagman, E. Dejardin, and D. R. Green.** 2006. Glycogen synthase kinase-3 regulates mitochondrial outer membrane permeabilization and apoptosis by destabilization of MCL-1. Mol. Cell **21:**749–760.
20. **McArdle, F., D. M. Pattwell, A. Vasilaki, A. McArdle, and M. J. Jackson.** 2005. Intracellular generation of reactive oxygen species by contracting skeletal muscle cells. Free Radic. Biol. Med. **39:**651–657.
21. **Miwa, S., and M. D. Brand.** 2003. Mitochondrial matrix reactive oxygen species production is very sensitive to mild uncoupling. Biochem. Soc. Trans. **31:**1300–1301.
22. **Miyazaki, T., L. Neff, S. Tanaka, W. C. Horne, and R. Baron.** 2003. Regulation of cytochrome c oxidase activity by c-Src in osteoclasts. J. Cell Biol. **160:**709–718.
23. **Mukhopadhyay, P., M. Rajesh, G. Hasko, B. J. Hawkins, M. Madesh, and P. Pacher.** 2007. Simultaneous detection of apoptosis and mitochondrial superoxide production in live cells by flow cytometry and confocal microscopy. Nat. Protoc. **2:**2295–2301.
24. **Oakes, S. A., J. T. Opferman, T. Pozzan, S. J. Korsmeyer, and L. Scorrano.** 2003. Regulation of endoplasmic reticulum Ca2+ dynamics by proapoptotic BCL-2 family members. Biochem. Pharmacol. **66:**1335–1340.
25. **Obexer, P., K. Geiger, P. F. Ambros, B. Meister, and M. J. Ausserlechner.** 2007. FKHRL1-mediated expression of Noxa and Bim induces apoptosis via the mitochondria in neuroblastoma cells. Cell Death Differ. **14:**534–547.
26. **Petros, J. A., A. K. Baumann, E. Ruiz-Pesini, M. B. Amin, C. Q. Sun, J. Hall, S. Lim, M. M. Issa, W. D. Flanders, S. H. Hosseini, F. F. Marshall, and D. C. Wallace.** 2005. mtDNA mutations increase tumorigenicity in prostate cancer. Proc. Natl. Acad. Sci. USA **102:**719–724.
27. **Piccoli, C., S. Scacco, F. Bellomo, A. Signorile, A. Iuso, D. Boffoli, R. Scrima, N. Capitanio, and S. Papa.** 2006. cAMP controls oxygen metabolism in mammalian cells. FEBS Lett. **580:**4539–4543.
28. **Prabu, S. K., H. K. Anandatheerthavarada, H. Raza, S. Srinivasan, J. F. Spear, and N. G. Avadhani.** 2006. Protein kinase A-mediated phosphorylation modulates cytochrome c oxidase function and augments hypoxia and myocardial ischemia-related injury. J. Biol. Chem. **281:**2061–2070.
29. **Rennefahrt, U., M. Janakiraman, R. Ollinger, and J. Troppmair.** 2005. Stress kinase signaling in cancer: fact or fiction? Cancer Lett. **217:**1–9.
30. **Rizzuto, R., P. Pinton, D. Ferrari, M. Chami, G. Szabadkai, P. J. Magalhaes, F. Di Virgilio, and T. Pozzan.** 2003. Calcium and apoptosis: facts and hypotheses. Oncogene **22:**8619–8627.
31. **Schinzel, A., T. Kaufmann, and C. Borner.** 2004. Bcl-2 family members: integrators of survival and death signals in physiology and pathology. Biochim. Biophys. Acta **1644:**95–105.
32. **Schulze, A., K. Lehmann, H. B. Jefferies, M. McMahon, and J. Downward.** 2001. Analysis of the transcriptional program induced by Raf in epithelial cells. Genes Dev. **15:**981–994.
33. **Scorrano, L., S. A. Oakes, J. T. Opferman, E. H. Cheng, M. D. Sorcinelli, T. Pozzan, and S. J. Korsmeyer.** 2003. BAX and BAK regulation of endoplasmic reticulum Ca2+: a control point for apoptosis. Science **300:**135–139.
34. **Setsukinai, K., Y. Urano, K. Kakinuma, H. J. Majima, and T. Nagano.** 2003. Development of novel fluorescence probes that can reliably detect reactive oxygen species and distinguish specific species. J. Biol. Chem. **278:**3170–3175.
35. **Thastrup, O., P. J. Cullen, B. K. Drobak, M. R. Hanley, and A. P. Dawson.** 1990. Thapsigargin, a tumor promoter, discharges intracellular Ca2+ stores by specific inhibition of the endoplasmic reticulum Ca2(+)-ATPase. Proc. Natl. Acad. Sci. USA **87:**2466–2470.
36. **Troppmair, J., J. T. Bruder, H. Munoz, P. A. Lloyd, J. Kyriakis, P. Banerjee, J. Avruch, and U. R. Rapp.** 1994. Mitogen-activated protein kinase/extracellular signal-regulated protein kinase activation by oncogenes, serum, and 12-O-tetradecanoylphorbol-13-acetate requires Raf and is necessary for transformation. J. Biol. Chem. **269:**7030–7035.
37. **Troppmair, J., and U. R. Rapp.** 2003. Raf and the road to cell survival: a tale of bad spells, ring bearers and detours. Biochem. Pharmacol. **66:**1341–1345.
38. **Ueda, S., H. Masutani, H. Nakamura, T. Tanaka, M. Ueno, and J. Yodoi.** 2002. Redox control of cell death. Antioxid. Redox Signal. **4:**405–414.
39. **von Gise, A., P. Lorenz, C. Wellbrock, B. Hemmings, F. Berberich-Siebelt, U. R. Rapp, and J. Troppmair.** 2001. Apoptosis suppression by Raf-1 and MEK1 requires MEK- and phosphatidylinositol 3-kinase-dependent signals. Mol. Cell. Biol. **21:**2324–2336.
40. **Wang, H. G., U. R. Rapp, and J. C. Reed.** 1996. Bcl-2 targets the protein kinase Raf-1 to mitochondria. Cell **87:**629–638.
41. **Waring, P.** 2005. Redox active calcium ion channels and cell death. Arch. Biochem. Biophys. **434:**33–42.
42. **Zamzami, N., P. Marchetti, M. Castedo, D. Decaudin, A. Macho, T. Hirsch, S. A. Susin, P. X. Petit, B. Mignotte, and G. Kroemer.** 1995. Sequential reduction of mitochondrial transmembrane potential and generation of reactive oxygen species in early programmed cell death. J. Exp. Med. **182:**367–377.
43. **Zebisch, A., and J. Troppmair.** 2006. Back to the roots: the remarkable RAF oncogene story. Cell. Mol. Life Sci. **63:**1314–1330.
44. **Zhong, J., J. Troppmair, and U. R. Rapp.** 2001. Independent control of cell survival by Raf-1 and Bcl-2 at the mitochondria. Oncogene **20:**4807–4816.
45. **Zhu, L. P., X. D. Yu, S. Ling, R. A. Brown, and T. H. Kuo.** 2000. Mitochondrial Ca(2+)homeostasis in the regulation of apoptotic and necrotic cell deaths. Cell Calcium **28:**107–117.
46. **Zorov, D. B., C. R. Filburn, L. O. Klotz, J. L. Zweier, and S. J. Sollott.** 2000. Reactive oxygen species (ROS)-induced ROS release: a new phenomenon accompanying induction of the mitochondrial permeability transition in cardiac myocytes. J. Exp. Med. **192:**1001–1014.